ELSEVIER

Journal of Nuclear Materials 246 (1997) 165–170

journal of nuclear materials

Investigation of impurity deposition on plasma facing component using electron beam technique

F.C. Sze *, R. Doerner, S. Luckhardt, R.W. Conn

Fusion Energy Research Program, University of California - San Diego, 9500 Gilman Drive, La Jolla, CA 92093-0417, USA

Received 27 December 1996; accepted 28 April 1997

Abstract

In experiments in PISCES-B facility we have observed carbon film formation on beryllium substrates after hydrogen plasma exposure. The sources of the carbon are gaseous impurities in the vacuum system, which also exist in a fusion reactor such as the International thermonuclear experimental reactor (ITER). Thin film formation, resulting from electron-impurity interactions, is studied using a focused electron beam. Initial results show that carbon films are readily formed on beryllium surface in a range of power densities from two kilowatts to over one megawatt per square meter. Electron beam experiments on silicon and tungsten substrates, under the same conditions, do not result in carbon film formation. Microanalyses using scanning electron microscopy, Energy Dispersive X-ray spectroscopy and Raman are presented. © 1997 Elsevier Science B.V.

1. Introduction

Thin film formation on plasma facing materials (PFMs) is an important subject in fusion reactor development because surface coatings will affect the lifetime of the plasma facing component, the tritium inventory, and the tritium recycling. Beryllium, tungsten and carbon are the three primary plasma facing materials in the current design of the International Thermonuclear Experimental Reactor (ITER) [1]. Beryllium is used as the first wall material in the fusion reactor. It is chosen because it is a low-Z material. Thus it has less fuel dilution effect on the performance of the fusion reactor [2]. Tungsten and carbon composites are being used in the divertor region because of their high melting temperatures. Erosion of these three materials in the edge plasma generates mobile particles in the vacuum chamber. These particles may migrate to other parts of the fusion reactor, where they may be ionized and re-deposited to form a film on the plasma facing component. The deposited carbon film not only affects the sputtering yield of the plasma facing material, but also acts as a depository for the isotopes during the D–T shots. Investigation of beryllium in the PISCES-B facility has observed impurity deposition on the beryllium surface after hydrogen plasma exposure [3]. Using a weight loss measurement, a reduction of sputtering yield of the PFM has been observed [4]. Auger electron spectroscopy (AES) of the plasma exposed beryllium surface showed a mixture of impurities, such as carbon and oxygen on the substrate surface. These earlier experiments used as-received beryllium samples, which had a surface roughness of several micrometers. This investigation uses polished beryllium disks so that deposited films can easily be observed and analyzed.

When ions reach the surface of the plasma facing material, several events can take place. The ions can bounce back as neutral species without kicking off surface atoms. If they have sufficient energies, they can break loose the surface atoms, a process known as surface sputtering. The ions can react with the surface atoms to form gaseous products, a process known as etching. The ions can also stick on the substrate surface to form a film. In the case of energetic ions, implantation will take place. All these events can happen at the same time in a plasma process.

* Corresponding author. Tel.: +1-619 534 2975; fax: +1-919 534 7716; e-mail: dsze@ucsd.edu.

PII S0022-3115(97)00141-4

Most plasma processes involve the measurement of parameters such as gaseous composition, surface temperature, ion and electron energy distributions and plasma density. Measurements of these parameters, however, do not help to provide the physical picture of the deposition process. Breaking down the plasma–surface interaction into deposition and etching components is one approach to study plasma–material interactions. When the deposition rate exceeds the etching rate, films will be formed.

Electron beam assisted techniques have been used for different metal films deposition [5–11]. Most of the processes used metallic carbonyls such as osmium, ruthenium [7], tungsten [5,8] and chromium [5]. The substrates were kept below room temperature. The substrate materials used were mostly silicon, silicon nitride and gallium arsenide. Fine features, which consisted of carbon and oxygen, were formed by using a combination of Gallium ion implantation and electron beam techniques [12]. This paper reports the initial results of electron beam deposition of carbon films on beryllium at room temperature without ion implantation. Local temperature, due to the electron beam heating, on the substrate is analyzed using the method described by Meingalis [13]. The source of carbon in the vacuum system is analyzed by a quadrupole mass analyzer. The electron beam process is also applied to silicon and tungsten substrates under the same conditions. Surface microanalyses of the deposited films are performed by using scanning electron microscopy and energy dispersive X-ray spectroscopy. Raman measurements of the electron beam deposited carbon films are also performed.

2. Experiments

2.1. Experiments in PISCES-B facility

The PISCES-B facility is a clean room facility designed for beryllium experiments. Fig. 1 shows the schematic drawing of the vacuum system. It consists of a plasma source region, a main chamber and a loading chamber. The plasma source is a dc discharge consists of a LaB_6 cathode with hot tungsten filaments on its back side. Two turbomolecular pumps with an effective pumping speed of 6500 l/s are attached to the vacuum chamber. The main chamber is surrounded by three electromagnetic coils, which generate a coaxial magnetic field along the axis of the vacuum system with a field strength around 500 G. Typically, a 5 cm diameter plasma column is formed along the axis of the vacuum chamber. A fast scanning double-Langmuir probe is used to measure the plasma temperatures and densities in the radial direction. Infrared pyrometer is used to monitor the surface temperature of the sample. The plasma performance of the PISCES-B facility has been described previously [4].

The samples are polished grade S-65B beryllium disks. Each has a diameter of 2.54 cm and a thickness of 1.5 mm.

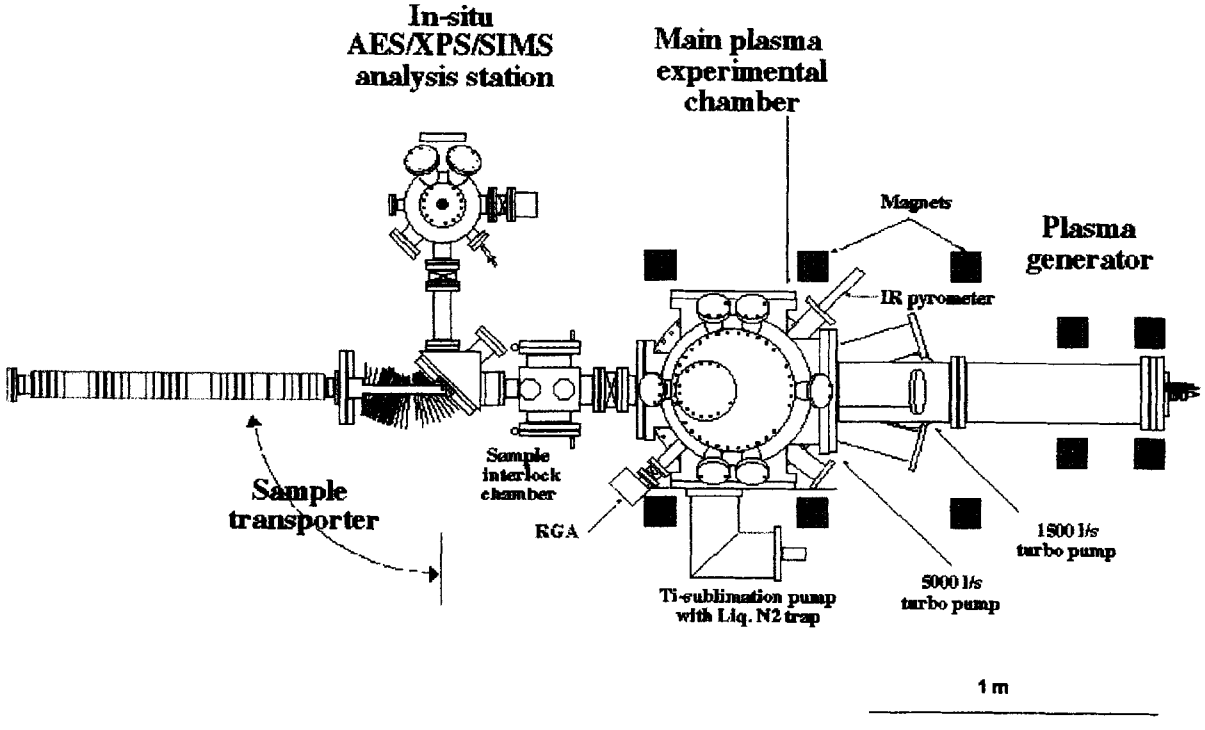

Fig. 1. PISCES-B facility.

It is clamped onto a water-cooled sample holder whose temperature is controlled by the water flow rate. An AMETEK DYCOR residual gas analyzer (RGA) is attached to the main vacuum chamber to measure the partial pressures of the residual gases. The base pressure of the system is 4×10^{-5} Pa. The operating pressure during the plasma exposure is about 1.33×10^{-2} Pa. The input gas is typically deuterium or hydrogen. The sample was heated up by the plasma to about 923 K and is held at that temperature for 30 min. No dc bias is applied to the sample. The floating potential is negative 100 V during plasma exposure.

2.2. Experiment using focused electron beam

A JEOL T330A SEM is used for the electron beam deposition experiments. The energy of the electron beam can be adjusted from 0.5 keV to 30 keV. During the deposition process, the beam is focused to a small area on the beryllium surface. Each polished beryllium sample is mounted on a movable stage which is electrically grounded. The temperature of the sample is 300 K. The magnitude of the electron beam current can be varied from 100 pA to 10 nA. Depending on the size of the sweeping area, the power densities vary from several kilowatts per square meter to over a megawatt per square meter. A Balzer QMA 064 quadrupole gas analyzer is used to measure the partial pressures of the gaseous impurities in the vacuum chamber.

3. Results and discussion

3.1. Impurities in vacuum systems

Fig. 2 shows the typical vacuum conditions measured by the RGA in PISCES-B at base pressure. It shows that the major impurities in the vacuum chamber are nitrogen (14, 28 amu), oxygen (16, 32 amu) and water (17, 18 amu). Using the ratios between the major peaks and the minor peaks in water and oxygen [14], the contributions of the two impurities towards the 16-amu peak are calculated. It is found that there is no methane (16 amu) in the vacuum chamber. Using the technique, the amount of nitrogen (28 amu) is calculated from the 14-amu peak. It is determined that the amount of carbon monoxide, whose mass is also 28 amu, is negligible. There is a small amount of argon (40 amu) and carbon dioxide (44 amu). The vapor pressure of the carbon dioxide measured is 3.2×10^{-7} Pa.

As the cathode of the plasma source in PISCES-B heats up, impurities from the hot cathode due to out-gassing increases the magnitude of the peak at 28 amu. Since the magnitude at 14 amu does not increase much, it is determined that the out-gassing species contain mainly carbon monoxide. How steady and how much carbon monoxide is coming out of the hot cathode during the experiment

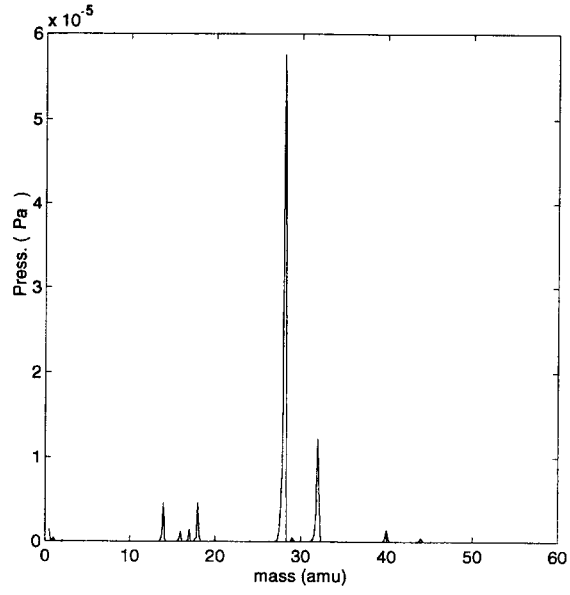

Fig. 2. RGA data in PISCES B.

remains to be determined. Since most RGAs do not indicate correct partial pressures at 1.33×10^{-2} Pa pressure, a high pressure quadrupole gas analyzer is needed in the future to trace the impurities during the plasma exposure. Assuming that the contribution to the 28 amu peak from the hot cathode is carbon monoxide and the amount stays the same throughout the experiment, a rough estimation of total amount of carbon impurities during plasma bombardment is about 0.5%. This is not a small number because it is well known that a level of 1% methane is sufficient to grow diamond film in a hydrogen plasma [15].

The vacuum conditions of the SEM is similar to the PISCES-B, but has a higher virtual leak rate. The base pressure is 4×10^{-3} Pa. However, since there is no hot cathode and known source for carbon monoxide, the only possible source of carbon species is carbon dioxide, which has a partial pressure of 8×10^{-6} Pa.

Fig. 3. Carbon deposition on beryllium.

Fig. 4. Convoluted carbon film on beryllium.

3.2. Thin film formation in PISCES-B facility

Figs. 3 and 4 show the scanning electron micrographs of carbon films formed on the beryllium surface after hydrogen plasma exposure in PISCES-B. Fig. 3 shows a broken carbon film formed on top of the beryllium substrate. Fig. 4 shows a convoluted carbon film on the right side of the electron micrograph.

The composition of the film is analyzed using KEVEX energy dispersive X-ray (EDX) analysis system. The EDX system is equipped with a quantum window detector which is capable of detecting elements from boron to uranium, based on the x-ray emissions due to transitions from the excited states to the ground states. Each element has its emission signature. Fig. 5 shows the EDX spectrum of the deposited film on beryllium, as shown in Fig. 3. It shows an energy peak at 0.290 keV, which is the characteristics X-ray emission from carbon. The film shown in Fig. 4 also has similar EDX spectrum, indicating that the convoluted film is also composed of carbon.

3.3. Electron beam assisted carbon deposition

The carbon films deposited in PISCES-B are formed under a constant bombardment of electrons and ions from the plasma. Moreover, any ions in the plasma will be accelerated towards the substrate surface by the sheath potential. Typical energies are in the range of 100 eV. These energetic ions are sufficient to cause surface sputtering. Keeping the incident ion energy to less than one eV will prevent sputtering from taking place. To keep the ions from gaining any energy, pre-sheath and sheath potentials have to be eliminated. That means a non-plasma environment is needed. This condition can be achieved by exposing neutral species to an energetic electron beam. The electrons will ionize the neutrals to generate ions at energies around one half electron-volt, which is the typical ion energy in the bulk of most laboratory plasmas [16]. According to TRIM calculations [17], the trapping coefficient of an incoming ion increases when the ion energy decreases. At the same time, the sputtering yield drops. At one eV energy level and below, the ions will hardly penetrate into the substrate. It can only stay on the surface. It is also necessary to point out that the amount of ions in this case is orders of magnitude less than the electrons compared with a steady state plasma, in which ions and electrons are reaching the surface at the same rate. Thus the deposition rate is primarily determined by the amount of impurities in the vacuum chamber.

Using a 5 keV electron beam, carbon patterns are deposited on beryllium surfaces during the electron beam exposure. Fig. 6 shows an electron beam deposited carbon dot, formed on top of a beryllium grain after 45 min of exposure. The carbon dot has a diameter of about one micrometer. Its EDX spectrum is similar to the one shown in Fig. 5, verifying that the deposited material is carbon.

To study the effect of power density on film growth, different power densities are tested. A constant electron beam current of 157 pA is scanned across different areas for half an hour. Table 1 lists the range of power densities used in these experiments. At each of these power densities, a carbon film is deposited. Fig. 7 shows the resulting carbon patterns on the beryllium.

As shown in Fig. 7, the carbon dots for A6, A7 and A8

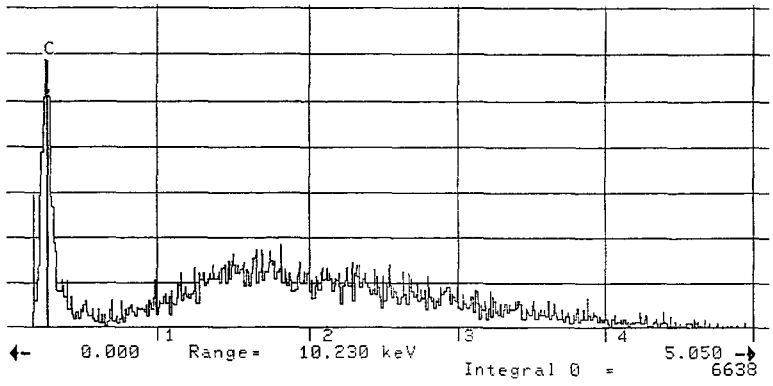

Fig. 5. EDX analysis of deposited material.

Fig. 6. Carbon dot on beryllium.

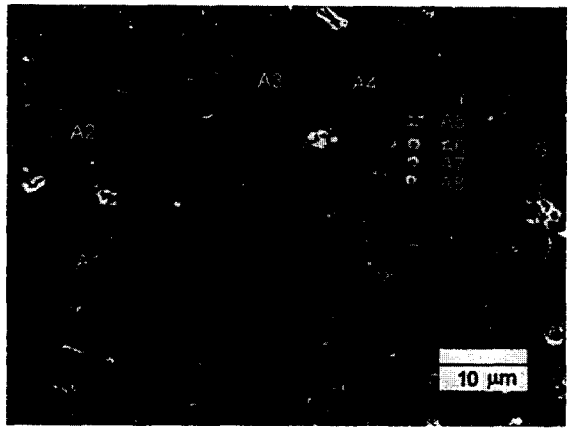

Fig. 7. Electron beam deposited carbon films at different power densities. (A1) 2 kW/m^2, (A2) 7.9 kW/m^2, (A3) 17.7 kW/m^2, (A4) 96 kW/m^2, (A5) 196 kW/m^2, (A6) 786 kW/m^2, (A7) 1.8 mW/m^2, and (A8) 3.1 MW/m^2.

are similar in size. This is because of the inability in the electron optics to manipulate the electron beam at submicron scales. Instead of being a rectangular pattern as A5 in Fig. 7, circular dots are formed. Thus, the actual power densities for A7 and A8 are less than the calculated values. The deposited films are not visible under the optical microscope. They are too small and thin for thickness measurement. However, from Fig. 7, it is shown that the thickness of the deposited film increases as the power density increases. At high power density, the carbon atoms are concentrated on a smaller area. Thus a thicker film is formed.

Using the radial heat flow model suggested by Meingalis [13], it is found that there is negligible temperature difference between the area exposed to the electron beam and the bulk of the beryllium substrate. For example, a beam energy of 5 keV with current density at 500 A/m^2 and a spot size of 1 μm, the temperature difference is only 0.07 K. Such small temperature difference is because beryllium has good thermal properties [18]. To achieve a temperature difference of 100 K between the exposed area and the bulk, the electron current has to be increased by about 1500 times, which is not achievable in this experimental setup.

Similar electron beam experiments are also performed on tungsten and silicon substrates. However, no carbon film is detected. There are several possible reasons why carbon films form so readily on beryllium, but not on tungsten and silicon. From published data [18,19], the diffusion coefficient of carbon in beryllium is more than several orders of magnitude higher than those in tungsten and silicon. It means that the deposited carbon can diffuse faster into beryllium under the same temperature than in tungsten and silicon. Moreover, beryllium is also chemically more active than silicon and tungsten.

Table 1
Power density level in e-beam deposition

Carbon pattern in Fig. 1	Calculated power density (kW/m^2)
A1	2
A2	7.9
A3	17.7
A4	96
A5	196
A6	786
A7	(1768)
A8	(3144)

The roles of electron beam in the deposition process thus are: (1) to ionize the neutral impurities to form ions, (2) to pull the ions to the surface of the substrate, and (3) to provide energy for carbon diffusion and bonding between carbon atoms. It is believed that the first two roles are the major roles. Only when a high current density is used, the last role will be significant.

Another observation is that water and oxygen are also present in the vacuum system. Their partial pressures are higher than the partial pressure of carbon dioxide. Dissociation and ionization of these three species will produce oxygen ions, which can react with beryllium to form oxide. The ionization rate coefficients for oxygen and carbon are similar [20]. However, there is no growth of oxide during the electron beam deposition process. One reason is that oxidation of beryllium takes place only at high temperature [21–23]. At room temperature, oxygen ions reach the surface and bounce off as neutrals. Thus there is no growth of an oxygen peak (0.523 keV) in the EDX spectrum.

The quality of the electron beam deposited carbon is examined using a Renishaw Raman Microscope. Fig. 8 shows the Raman shift of a carbon film, deposited at a power density of 16 kWm^{-2} at room temperature. It shows a diamond-like carbon in the deposited film. Chang-

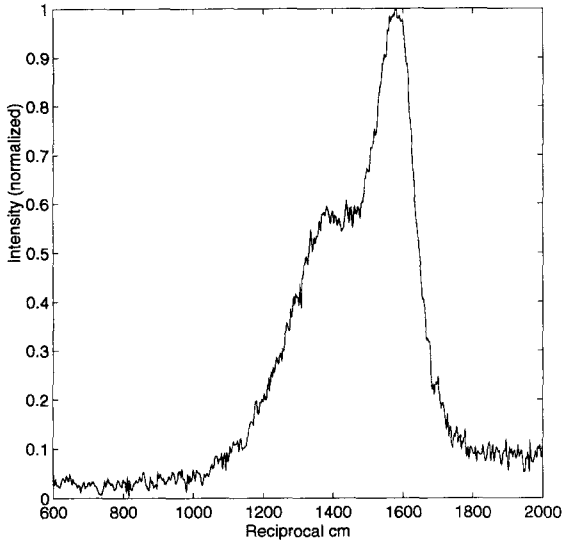

Fig. 8. Raman measurement on electron beam deposited carbon.

ing the power density to 1.6 MWm^{-2} also results in similar spectrum.

4. Summary

Carbon films are observed on beryllium surfaces after plasma exposure in PISCES-B facility at 923 K. The source of carbon is the impurities in the vacuum system which is estimated to be 0.5%. The interaction of carbon dioxide impurity and energetic electrons is studied using a focused electron beam. The technique demonstrates that carbon films are readily deposited on beryllium substrate at room temperature. Because of the high thermal conductivity in beryllium, variation of power density only results in change of film thickness as depicted in Fig. 7. Similar experiments on silicon and tungsten do not yield carbon film formation. The electron beam technique does not affect the substrate temperature. Thus the technique is useful for studying impurity deposition on plasma facing materials at different electron energies and substrate temperatures (by external substrate heating).

Acknowledgements

The authors would like to express their thanks to L. Chousal, P. Luong and G. Gunner for their laboratory support. The Raman measurement is made possible with the help from Professor Talke for allowing one of the authors (F.C.S.) to use his Raman analyzer. This research work is supported by a grant from the US Department of Energy numbered DE-FG03-95ER-54301.

References

[1] International Thermonuclear Experimental Reactor, DOE/ER-ITER-0004, 1993.
[2] R.W. Conn, Fusion Eng. Des. 14 (1991) 81.
[3] Y. Hirooka, J. Won, R. Boivin, D.(F.C.) Sze, V. Neumoin, J. Nucl. Mater. 230 (1996) 173.
[4] J. Won, PhD thesis, University of California (1996).
[5] R.W. Bigelow, J.G. Black, C.B. Duke, W.R. Salaneck, H.R. Thomas, Thin Solid Films 94 (1982) 233.
[6] S. Matsui, K. Mori, J. Vac. Sci. Technol. B4 (1) (1986) 299.
[7] V. Scheuer, H. Koops, T. Tschudi, Microelectron. Eng. 5 (1986) 423.
[8] H.W.P. Koops, R. Weiel, D.P. Kern, J. Vac. Sci. Technol. B6 (1) (1988) 477.
[9] T. Ichihashi, S. Matsui, J. Vac. Sci. Technol. B6 (6) (1988) 1869.
[10] A. Ishibashi, K. Funato, Y. Mori, J. Vac. Sci. Technol. B9 (1) (1991) 169.
[11] K.L. Lee, M. Hatzakis, J. Vac. Sci. Technol. B7 (6) (1989) 1941.
[12] H. Ximem, P.E. Russell, Ultramicroscopy 42–44 (1992) 1526.
[13] J. Meingalis, J. Vac. Sci. Technol. B5 (2) (1987) 469.
[14] M.J. Drinkwine, D. Lichtman, Partial Pressure Analyzers and Analysis, AVS Monograph Series, AVS Press, p. 35.
[15] J. Zhang, PhD thesis, Michigan State University (1993).
[16] G. King, F.C. Sze, P. Mak, T.A. Grotjohn, J. Asmussen, J. Vac. Sci. Technol. A10 (4) (1992) 1265.
[17] J.F. Ziegler, J.P. Biersack, U. Littmark, The Stopping and Range of Ions in Solids (Pergamon, New York, 1980).
[18] R.C. Weast, Handbook of Chemistry and Physics (CRC, Boca Raton, FL, 1986).
[19] N.K. Lashchuk, V.G. Tkachenko, A.V.I. Trefilov, Sov. Phys. Dokl. 26 (6) (1981) 608.
[20] K.K. Bell, H.B. Gilbody, J.G. Hughes, A.E. Kingston, F.J. Smith, Atomic and Molecular Data for Fusion, Part I, Recommendation Cross Sections and Rates for Electron Ionization of Light Atoms and Ions, Culham Laboratory, 1982.
[21] S.J. Gregg, R.J. Hussey, W.B. Jepson, J. Nucl. Mater. 2 (3) (1960) 225.
[22] S.J. Gregg, R.J. Hussey, W.B. Jepson, J. Nucl. Mater. 3 (2) (1961) 175.
[23] S.J. Gregg, R.J. Hussey, W.B. Jepson, J. Nucl. Mater. 4 (1) (1961) 46.